

Detection of Moving Radar Targets in Clutter

LARS-HENNING ZETTERBERG

Research Institute of National Defence, Stockholm, Sweden

The moving target indicator is investigated for threshold power and visibility in clutter. In search for improvements, electronic scanning of the antenna beam is proposed and a detector is considered combining more than two pulses at a time.

1. INTRODUCTION

In the presence of ground echoes, the detection of radar targets is aggravated. It may be made efficient by taking advantage of the difference in radial velocity of the target and of the reflecting objects on the ground. One such scheme is the moving target indicator (MTI) discussed by Ridenour (1947) and Grisetti *et al.* (1956) among others. The pulses are received with the phase information retained and the detector subtracts two successively received pulses. For a moving target, the doppler shift of the carrier frequency will change the phase of the received pulse whereas a ground echo will leave it essentially unchanged, the pulses thus canceling in the detector output. For two reasons, the cancellation is not perfect. One reason is small movements of some ground objects, the other is the antenna rotation causing slightly different ground areas to be illuminated by successive pulses. From the detector, the signal is fed to a cathode ray tube used as a plane position indicator (PPI).

Following Lawson and Uhlenbeck (1950), we shall apply the deflection criterion to calculate the detectability of targets. The spot brightness on the PPI is observed after one angular sweep of the antenna past the point where the target is supposed to be located and the brightness is compared to that of the surrounding areas. If the difference is large enough a target will be indicated. More specifically a target is said to be detectable if the observed difference on the average is some number k larger than the fluctuation in brightness caused by the clutter alone. The smallest signal power for which this is true is called the threshold signal power for detection.

One object of the study is to calculate this power for radar equipped with MTI detector when the detection is limited by ground echoes, precipitation, sea reflections, or aluminum foils (chaff). Clutter is used as the generic term for those echoes. The study parallels what is done by Lawson and Uhlenbeck (1950) on A-scope and PPI observation where target detection is limited by internal noise. The clutter signal shows a statistical dependence from one pulse to another and in this sense differs from the internal noise signal. In the analysis it is compensated for by simplifying assumptions about the detector and the PPI screen brightness characteristics. The performance of the radar equipped with MTI detector is compared to a radar without one and the choice of parameters is discussed for the two cases.

Another purpose is to discuss how the detection of moving targets may be further improved. The signal detector may combine the received signals from more than two pulses and hence take advantage of the statistical properties of the clutter signal to make the subtraction circuits more effective. As an alternative method, a scheme is proposed which applied to a radar with MTI detector avoids the limitations due to the rotation of the antenna. With the antenna itself rotating, the movements of the beam are momentarily compensated for by electronic means.

The radar parameters that primarily appear are the beamwidth ϕ_0 [radian], the antenna rotation [radian/sec], the pulse repetition frequency f_p [cycles/sec], or the pulse period $T = 1/f_p$ [sec] and the wavelength λ [meter]. They are grouped together and define two new parameters: n , the number of hits per beamwidth, and n_p , the number of pulse periods on one doppler period. This last number is calculated with the velocity v_e characterizing the movements of the reflecting clutter objects and f_{de} denoting the corresponding doppler frequency

$$n = \phi_0/\omega_a T; \quad n_p = f_p/f_{de} = f_p \lambda / 2v_e \quad (1)$$

The transmitted pulse is considered rectangular and the video and IF bandwidths are wide enough not to disturb the pulse shape seriously. The length of the transmitted pulse affects the received clutter power and thus enters into the threshold signal power while this is independent of the power of the transmitted pulse.

2. A STATISTICAL MODEL OF THE CLUTTER SIGNAL

The properties of an individual reflecting object are given by its location, motion, and reflection coefficient. For our purpose it is sufficient

to know θ , the azimuth angle; ρ , the phase of the reflected signal at time $t = 0$ [This is the sum of the phase of the reflection coefficient and the phase due to the radial location.]; f_d , the doppler frequency $2v/\lambda$, with v the radial velocity towards the station; z , the absolute value of the reflection coefficient.

With a transmitted carrier frequency f , the received signal has a frequency $f + f_d$ due to the doppler-shift. Let $G(\phi)$ describe the antenna diagram in voltage for two-way transmission. The clutter signal from one object then will be

$$zG(\theta - \omega_a t) \sin [2\pi(f + f_d)t + \rho]$$

The entire clutter signal is the sum of a large number of terms from individual reflectors and may be written

$$x(t) \cos 2\pi ft + y(t) \sin 2\pi ft$$

with

$$\begin{aligned} x(t) &= \sum_i z_i G(\theta_i - \omega_a t) \sin (2\pi f_{di} t + \rho_i) \\ y(t) &= \sum_i z_i G(\theta_i - \omega_a t) \cos (2\pi f_{di} t + \rho_i) \end{aligned} \quad (2)$$

At a specific time t , the series are summed over all reflectors within the illuminated area defined by the pulselength and the beamwidth of the antenna at the specified distance from the radar station.

The quantities θ , ρ , f_d , and z are all random variables about which the following assumptions are made [Lawson and Uhlenbeck (1950)]: (1) The reflectors are evenly distributed with a density q per radian within the pulselength. (2) The reflectors behave in a statistically independent manner. (3) z and ρ are independent. ρ has a rectangular distribution $(0, 2\pi)$. (4) No z_i dominates and the number of reflectors illuminated at the same time is large whereas the number of reflectors which leave or enter an illuminated area during the time between successive pulses is small. (5) The radial velocity is zero for a proportion $1 - a$ of reflectors whereas the rest move radially with a velocity that is normally distributed with mean v_m and variance v_e^2 . Although the number of reflectors is about the same from one pulse to another, some reflectors will come out of the beam and other enter into it as the antenna scans. In accordance with assumption (4), the number of reflectors which leave the beam because of their own movements is negligible.

3. PROPERTIES OF THE CLUTTER SIGNAL

From the assumptions, one can assert that $x(t)$ and $y(t)$ are normally distributed with zero mean and a variance equal to $\frac{1}{2}\sigma^2$, where

$$\sigma^2 = E\{z^2\} \sum_i G^2(\theta - \omega_a t)$$

may be interpreted as the clutter power received. The autocorrelation and crosscorrelation function of $x(t)$ and $y(t)$ may be expressed as

$$E\{x(t)x(t + \tau)\} = E\{y(t)y(t + \tau)\} = \frac{1}{2}\sigma^2\zeta(\tau)$$

$$E\{x(t)y(t + \tau)\} = -E\{x(t + \tau)y(t)\} = \frac{1}{2}\sigma^2\lambda(\tau)$$

with

$$\begin{aligned}\zeta(\tau) &= \frac{H(\tau)}{H(0)} \left[1 - a + a \cos(2\pi f_{dm}\tau) \exp \left\{ -\frac{1}{2} (2\pi f_{de}\tau)^2 \right\} \right] \\ \lambda(\tau) &= -\frac{H(\tau)}{H(0)} a \sin(2\pi f_{dm}\tau) \exp \left\{ -\frac{1}{2} (2\pi f_{de}\tau)^2 \right\}\end{aligned}\quad (3)$$

where f_{dm} and f_{de} are doppler frequencies computed with the mean velocity v_m and the standard derivation v_e , respectively. The notation

$$H(\tau) = \sum_i G(\theta_i - \omega_a t) G(\theta_i - \omega_a(t + \tau))$$

is introduced. On account of the assumptions of an even distribution of a large number of reflectors, $H(\tau)$ is independent of t and approximately

$$H(\tau) = q \int_{-\infty}^{\infty} G(x) G(x - \omega_a \tau) dx$$

For later use we record $H(\tau)$ for a special case of the antenna diagram, the Gaussian shape

$$G(\phi) = \exp \left\{ -\frac{\pi}{2} \left(\frac{\phi}{\phi_0} \right)^2 \right\}, \quad H(\tau) = q\phi_0 \exp \left\{ -\pi \left(\frac{\omega_a \tau}{2\phi_0} \right)^2 \right\} \quad (4)$$

The received clutter power then may be written

$$\sigma^2 = E\{z^2\} H(0) = qE\{z^2\} \phi_0 = w\phi_0 \quad (5)$$

where w is interpreted as the power density per radian within a pulse-length. The antenna diagram is normalized through ϕ_0 , such that the clutter power σ^2 is the product of w and ϕ_0 . In this study, the beam-width will be identified with ϕ_0 whereas a definition with the transmitted

TABLE I
EXPERIMENTAL VALUES OF a AND v_e

Clutter	Wind, mph	v_e , meters/sec	a
Wooded terrain	10	0.043	0.16
Wooded terrain	23	0.046	0.50
Wooded terrain	22	0.11	0.50
Wooded terrain	23	0.11	0.55
Wooded terrain	30	0.19	0.83
Wooded terrain	50	0.10	1.0
Chaff	≍ 10	0.25	1.0
Chaff	≍ 10	0.51	1.0
Chaff	≍ 10	0.67	1.0
Chaff	25	0.97	1.0
Rain echoes		1.4-2.8	1.0
Sea echoes		0.4-0.8	1.0

signal 3 db down corresponds to $1.33 \phi_0$. Table I contains values of a and v_e estimated out of Lawson and Uhlenbeck (1950) and Kerr (1951).

4. THE TARGET SIGNAL

The variations in amplitude of the return signal are generated by factors like long time change in aspect of sight, stochastic movements of the aircraft, and periodic vibrations in the structure. The phase of the target signal, defined relative to the transmitted carrier, depends upon the radial velocity of the aircraft and upon the phase of the reflection coefficient.

With the target in zero azimuth angle at time $t = 0$, the cosine and sine component of the return signal will be described as

$$x(t) = \xi(t)G(\omega at); \quad y(t) = \eta(t)G(\omega at) \quad (6)$$

where $\xi(t)$ and $\eta(t)$ are the recorded signal components with fixed antenna and the target in the center of the beam. A mathematical model will be assumed where $\xi(t)$ and $\eta(t)$ have no correlation when generated by two different pulses; that is,

$$E\{\xi(t)\xi(t + \nu T)\} = E\{\eta(t)\eta(t + \nu T)\} = 0$$

with ν a positive or negative integer and T the pulse interval. At one point in the analysis $\xi(t)$ and $\eta(t)$ will be assumed to be normally distributed with no crosscorrelation for any observations; that is,

$$E\{\xi(t)\eta(t + \nu T)\} = 0, \quad \nu = 0, \pm 1, \pm 2, \dots$$

The assumptions about zero correlation are rather strong but motivated, primarily, by the rapid phase change due to a high radial velocity. This means, at 10 cm wavelength, a doppler frequency many times the pulse frequency. A whole class of radial velocities must be considered and averaging over this class will tend to diminish the correlation for separate pulse returns.

5. RECEIVER CHARACTERISTICS

The transmitted pulse samples the target and clutter signal at times t_i with even intervals T , where the observations refer to a fixed radial distance from the radar station. Denote the sampled cosine and sine component of the received signal

$$x_i = x(t_i), \quad y_i = y(t_i) \quad (7)$$

The MTI detector will be considered sensitive to both phase and amplitude and thus will have no preceding limiter. The detector then forms the vector difference between the signals for successive pulses and produces the absolute value thereof. The sampled video signal is then defined by

$$u_i = [(x_i - x_{i-1})^2 + (y_i - y_{i-1})^2]^{1/2} \quad (8)$$

It is known (Grisetti *et al.*, 1955) that the clutter attenuation will be about 3 db less with the limiter removed. Assuming a target signal with constant amplitude, the threshold signal power will be affected by about the same amount. However in practice there are amplitude variations which partly compensate for the difference.

The spot brightness on the PPI is a result of summed contributions from several sweeps. The combined effect of the finite width of the electron beam and the integrating ability of the eye is postulated as a mechanism adding the brightness from a succession of sweeps weighted with coefficients k_i . When this is put into a formula the nonlinearity of a PPI screen will be included. The brightness v is related to the intensifier electrode voltage u as $v = u^p$ [Sponsler and Shader (1954) and RCA Tube Handbook] with p between 2 and 3. To simplify the computations the choice will be $p = 2$, which means that the spot brightness may be written as

$$v = \sum_{i=-\infty}^{\infty} k_i u_i^2 \quad (9)$$

Observing a target located in zero azimuth angle at time $t_0 = 0$, k_i should have large values for neighboring values of t_i . Particularly consider

$$k_i = K \left(\frac{i}{n_f} \right) = \exp \left\{ -\frac{\pi}{2} \left(\frac{i}{n_f} \right)^2 \right\} \quad (10)$$

with n_f characterizing the electron beamwidth and the integrating ability of the eye.

For a radar without MTI, expression (8) is replaced by

$$u_i = [x_i^2 + y_i^2]^{1/2} \quad (11)$$

6. THE THRESHOLD SIGNAL POWER FOR RADAR WITH MTI

The introduction explained what is considered a detectable target. With such a target the following inequality must be satisfied

$$\frac{E_{p_1}\{v\} - E_{p_0}\{v\}}{(E_{p_0}\{v^2\} - [E_{p_0}\{v\}]^2)^{1/2}} \geq k \quad (12)$$

The expectations are carried out with respect to the probability distributions p_1 and p_0 , which hold true when a target is present or absent, respectively.

$$\begin{aligned} S_1 &= E_{p_1}\{v\} - E_{p_0}\{v\} = s^2 \sum_i k_i [G^2(\omega_{at_i}) + G^2(\omega_{at_{i-1}})] \\ S_2^2 &= E_{p_0}\{v^2\} - [E_{p_0}\{v\}]^2 = \sigma^4 \sum_{ij} k_i k_j [B_{ij}^2 + C_{ij}^2] \end{aligned} \quad (13)$$

with

$$\begin{aligned} B_{ij} &= 2\zeta[(j-i)T] - \zeta[(j-i-1)T] - \zeta[(j-i+1)T] \\ C_{ij} &= 2\lambda[(j-i)T] - \lambda[(j-i-1)T] - \lambda[(j-i+1)T] \end{aligned}$$

These expressions will be further discussed when $v_m = 0$, that is, with zero mean radial velocity. This is true with ground echoes and presumably also with sea echoes. The results will apply also with rain and chaff when the receiver is equipped with an auxiliary oscillator to compensate for the doppler frequency due to the mean radial velocity. The assumption $v_m = 0$ implies $C_{ij} = 0$. With $G(\phi)$ and $K(x)$ smooth functions, n , n_p and n_f fairly large, the expressions for S_1 and S_2 may be evaluated as integrals. Approximately,

$$B_{ij} = -T^2 \zeta''[(j-i)T]$$

and

$$S_1 = 2s^2 n_f \int_{-\infty}^{\infty} K(x) G^2(\omega_a T n_f x) dx$$

$$S_2^2 = \sigma^4 T^3 n_f \iint_{-\infty}^{\infty} [\zeta''(y)]^2 K(x) K\left(x + \frac{y}{n_f T}\right) dx dy$$

The particular choice of $G(\phi)$ and $K(x)$ in (4) and (10) enables the integrations to be carried out. Introduce the notations

$$\xi = n/n_f \quad \eta^2 = 1 + 8\pi(n/n_p)^2, \quad \eta > 0$$

$$f(x, y) = \frac{1}{(x^2 + y^2 + 1)^{1/2}} \left[\frac{2y^2}{(x^2 + y^2 + 1)^2} + \left(\frac{y^2}{x^2 + y^2 + 1} - 1 \right) \left(\frac{1}{x^2 + y^2 + 1} - 1 \right) \right] \quad (14)$$

$$R(x, y, a) = (1 - a)^2 f(x, 1) + a^2 y^3 f(x/y, 1) + 2a(1 - a)y^2 f(x, y)$$

There is then

$$S_1 = 2 \sqrt{2} \frac{s^2 n}{(\xi^2 + 2)^{1/2}}$$

$$S_2^2 = \frac{\pi^2}{2} \cdot (w\omega_a T)^2 \frac{R(\xi, \eta, a)}{\xi} \quad (15)$$

with the special cases

$$R(\xi, \eta, 0) = f(\xi, 1)$$

$$R(\xi, \eta, 1) = \eta^3 f(\xi/\eta, 1)$$

Equality in (12) defines the signal threshold power $s^2 = s_m^2$, where

$$s_m^2 = \frac{k\pi}{4} \cdot \frac{w\omega_a T}{n} \left[\frac{\xi^2 + 2}{\xi} R(\xi, \eta, a) \right]^{1/2} \quad (16)$$

7. HOW THE RADAR PARAMETERS AFFECT THE THRESHOLD POWER. SUBCLUTTER VISIBILITY

We expect a certain value of the integration constant n_f to minimize the threshold power. Too small a value of n_f will appreciably diminish the response from the target while affecting the clutter signal less seriously. When n_f becomes large enough the target response has about reached its limit while the clutter signal continues to grow as more and more

sweeps are included in the integration. Accurate information about the integration is included in Fig. 1. The optimum value of n/n_f is found to be between $2^{1/2}$ and $(2 + \sqrt{7})^{1/2}$, the exact value depending on η and a , but the variation of the threshold power over this interval is fairly small for all combinations thereof. It is decided to use a fixed value of $n/n_f = 1.8$ when investigating the dependence on other parameters.

Varying the antenna beamwidth is formally equal to varying the number of hits per beamwidth with $\omega_a T$ fixed. It is apparent from Fig. 2 that with a variable component in the clutter signal, that is, $a > 0$ and $n_p < \infty$, there is a best choice of beamwidth in the sense of minimiz-

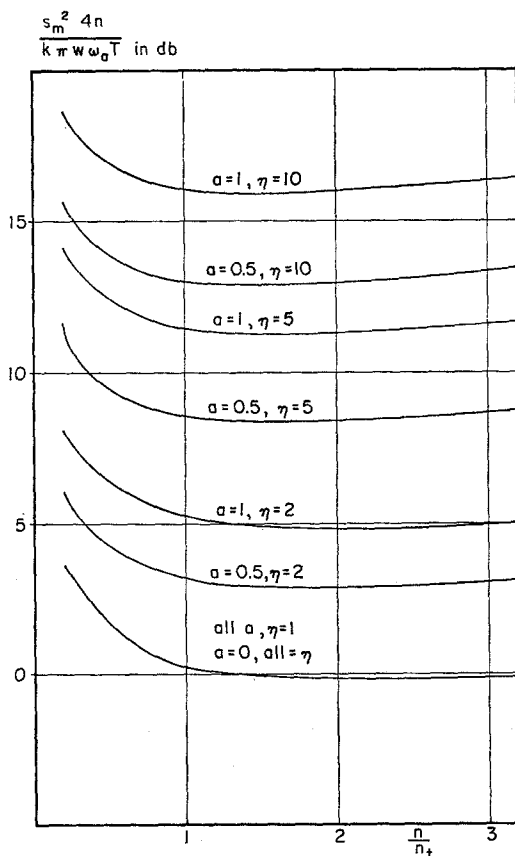


FIG. 1. Threshold signal power s_m^2 with MTI radar versus the reciprocal of n_f , the CRT integration constant.

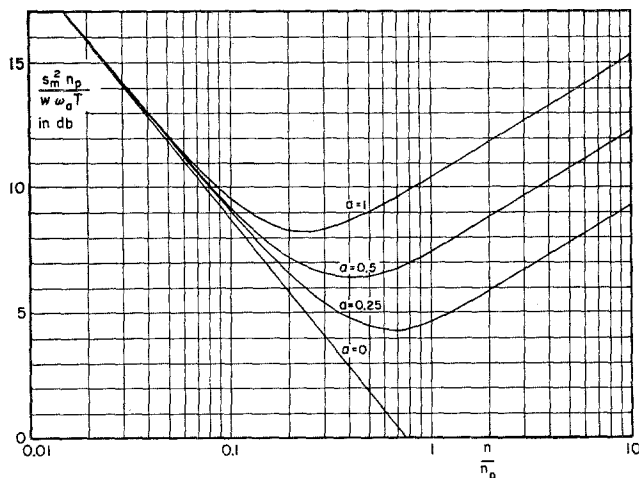


FIG. 2. The influence of antenna beamwidth ϕ_0 on the threshold signal power s_m^2 . Scale on horizontal axis, $n/n_p = \phi_0 f_{de}/\omega_a$.

ing the threshold power. As an example, consider a station with $\lambda = 0.1m$, $f_p = 1000$ cycles/sec, $\omega_a = 0.4\pi$ rad/sec (12 rpm), and a typical value for ground clutter of $n_p = 500$. With no fixed component in the ground clutter, that is, $a = 1$, the optimum choice corresponds to 118 hits per beamwidth. This means a beamwidth of 8.5° .

The threshold power is inversely proportional to the pulse repetition frequency squared because of an improved cancellation of the clutter.

As far as scanning is concerned a slow rotation favorably affects the threshold power. Studying the scanning rate ω_a when the beamwidth and pulse repetition frequency are fixed, is identical with varying the number of hits per beamwidth when these same parameters are fixed. Formally it is achieved by replacing $\omega_a T$ in (16) by ϕ_0/n . The formula then may be used to express the "subclutter" visibility, defined as the total clutter power $w\phi_0$ divided by the signal power s_m^2 , in which case the constant k is chosen equal to 9 (Lawson and Uhlenbeck, 1950).

$$\frac{w\phi_0}{s_m^2} = \frac{4}{k\pi} \cdot n^2 \left[\frac{\xi^2 + 2}{\xi} R(\xi, \eta, a) \right]^{-1/2} \quad (17)$$

Figure 3 has the subclutter visibility as a function of the number of hits per beamwidth but it is also possible to interpret as a diagram of $1/s_m^2$ against $1/\omega_a$.

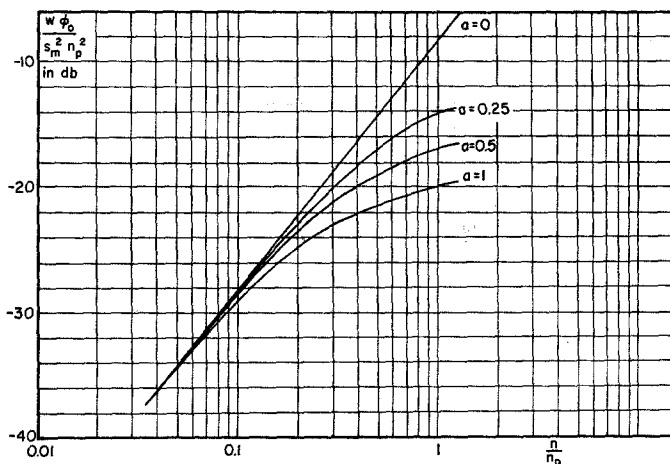


FIG. 3. Subclutter visibility $w \phi_0/s_m^2$ with MTI radar versus the number n of hits per beamwidth. Add $20^{10} \log n_p$ to ordinate to get visibility in db.

The diagram shows a quadratic dependence of visibility on the number of hits per beamwidth when the number is relatively small and a square root relation for larger values when $a > 0$. In the former case there is a strong correlation between all n signal values from the clutter. Then η is close to 1 and the cancellation of the clutter is limited by the antenna rotation. Larger n then means improved cancellation. In the latter case the n^2 -term dominates η and the correlation is small between the first and the n th signal sample, particularly when a is close to 1. The motion of the scatterers limits the cancellation. Increasing the number of pulses n through a longer observation time ϕ_0/ω_a means more and more weakly correlated signal samples added in the output. This explains the improvement in subclutter visibility with increasing \sqrt{n} as a result of post detector integration.

The wavelength enters into (16) through the variable η . The choice of wavelength controls if the scatters' motion or the antenna rotation limits the operation. When the motion effect dominates, a longer wavelength will decrease the threshold power, while otherwise the threshold power is very little affected by the wavelength. Transition between the two cases occurs when

$$\lambda = \sqrt{32\pi} \frac{\phi_0 v_e}{\omega_a}$$

This wavelength depends on the observation time ϕ_0/ω_a and on the velocity of the scatterers. With a short observation time, the formula indicates that a short wavelength may be used. However, there is then little advantage with an MTI detector, as will be shown in the following sections. An efficient MTI radar requires a long observation time and hence a long wavelength.

8. THRESHOLD POWER FOR THE NORMAL RADAR

The receiver characteristics are defined by Eqs. (9) and (11). Then

$$S_1 = E_{p_1}\{v\} - E_{p_0}\{v\} = s^2 \sum_i k_i G^2(\omega_a t_i)$$

The form of S_2^2 will be identical to that of (13) with the interpretation

$$B_{ij} = \zeta[(j - i)T], \quad C_{ij} = \lambda[(j - i)T]$$

Approximately when $n, n_p, n_f \gg 1$,

$$S_2^2 = \frac{\sigma^4 n_f}{T} \iint_{-\infty}^{\infty} \zeta^2(y) K(x) K\left(x + \frac{y}{n_f T}\right) dx dy$$

Integration will give

$$S_2^2 = 2(w\phi_0 n)^2 \frac{S(\xi, \eta, a)}{\xi}$$

where

$$S(x, y, a) = (1 - a)^2 g(x, 1) + \frac{a^2}{y} g(x/y, 1) + 2a(1 - a)g(x, y)$$

$$g(x, y) = \frac{1}{(x^2 + y^2 + 1)^{1/2}}$$

S_1 becomes, in the limit, half the value of that in (15) and hence the threshold power is

$$s_m^2 = kw\phi_0 \left[\frac{\xi^2 + 2}{\xi} S(\xi, \eta, a) \right]^{1/2} \quad (18)$$

Considering the extreme case of no motion of clutter there is no finite value of $\xi = n/n_f$ which minimizes the threshold power. The ratio should be taken as large as possible, which means that each single sweep will separately control the PPI brightness. This seems reasonable because the clutter acts as an extended fixed target while the aircraft is located

at a specific point and thus suffers in signal strength when it is off the radar beam.

Without a steady component of clutter, ν should be taken as large as possible if the scanning effects dominate; that is, $\eta^2 < 2$. The minimum value is then $kw\phi_0$. When the motion effects dominate, $\eta^2 > 2$ and there is a finite value of ξ which gives the threshold power a minimum

$$\sqrt[4]{2} \frac{kw\phi_0}{\sqrt{\eta}}, \quad \eta > \sqrt{2} \quad (19)$$

Additional material is included in Fig. 4.

The dependence on η in (19) is natural since η is a function of the observation time ϕ_0/ω_a and indeed proportional to it when the time is long enough. Formula (19) then expresses post detector integration.

A narrow beam will improve detection because less clutter power reaches the receiver. The beamwidth also enters through η and, with the motion effect dominating the threshold power, becomes proportional to the square root of the beamwidth and not to the beamwidth itself.

Equation (18) has the somewhat surprising result that the pulse repetition frequency does not affect the threshold power when the observation time has a fixed value. This is in contrast to detection in internal noise (Lawson and Uhlenbeck, 1950).

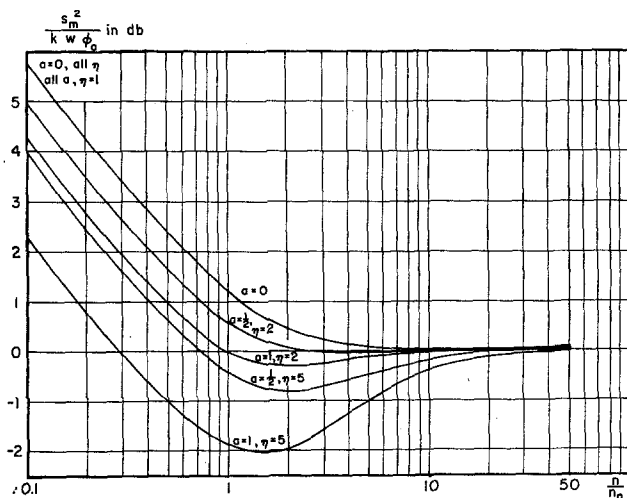


FIG. 4. Threshold signal power s_m^2 with normal radar versus the reciprocal of n_f , the CRT integration constant.

9. COMPARISON OF THRESHOLD POWER WITH AND WITHOUT MTI

The comparison is done with identical radar parameters except for a separate choice of filter constant for the PPI integration. The ratio of threshold power of the normal radar to that with MTI might be called the relative merit of MTI. In the extreme cases where $a = 0$ and $a = 1$ it is

$$\begin{aligned} r &= 1.32n^2 & a &= 0 \\ r &= 0.75 \frac{n^2}{\eta^{3/2}[f(1.8/\eta, 1)]^{1/2}} & a &= 1 \quad \text{and} \quad 1 \leq \eta < \sqrt{2} \quad (20) \\ r &= 0.89 \frac{n^2}{\eta^2[f(1.8/\eta, 1)]^{1/2}} & a &= 1 \quad \text{and} \quad \sqrt{2} \leq \eta \end{aligned}$$

The ratio depends primarily on the observation time and on the pulse repetition frequency. The motion of clutter limits the ratio to $0.049 n_p^2/a^2$ as the observation time is made longer. This result actually holds for an arbitrary proportion of variable clutter power (Fig. 5).

As an example a typical long-range and short-range radar is analyzed with respect to the MTI action in Table II. The wavelength is taken as 10 cm and the scatter velocity $v_e = 0.2$ meter/sec. In a high-resolution

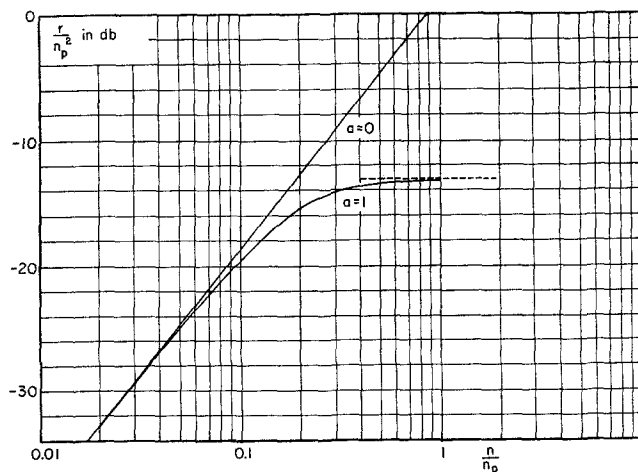


FIG. 5. Adding $20 \log n_p$ to the ordinate gives the difference in threshold power in db between the radar without and with MTI as a function of the number of hits per beamwidth n .

TABLE II
ANALYSIS FOR MTI ACTION

	Long range	Short range
Beamwidth, 3 db down	0.3°	1.5°
Scanning rate, rpm	6	6
Pulse repetition frequency, cycles/sec	300	1200
Relative merit, db	7	30.5
Subclutter visibility, db	-2.5	21

long-range station MTI would be of no use, but it improves detection considerably for a carefully designed short-range radar.

10. A GENERALIZED MTI DETECTOR

Let x_i and y_i with $i = 1, \dots, 2m + 1$ be the set of cosine and sine amplitudes of a coherent IF signal (7). Denote with \mathbf{z} the column vector

$$\{x_1, \dots, x_{2m+1}, y_1, \dots, y_{2m+1}\}$$

With no target present \mathbf{z} , is distributed according to $p_0(\mathbf{z})$; otherwise, \mathbf{z} is distributed according to $p_1(\mathbf{z}, s)$, with s^2 the target signal power unknown.

A test of the hypothesis "no target present" will be considered and based on one observation \mathbf{z} . The test procedure will be used as a detector and no integration on the PPI will be allowed. For simplicity only an odd number of pulses fed to the detector will be considered and the target, if present, will be in the center of the beam for the observation labeled $i = m + 1$. The special case of the target signal mentioned in Section 4 will be assumed; that is, $\xi(t)$ and $\eta(t)$ in (6) are normally distributed and there is no crosscorrelation. The test will be constructed under the assumption $s^2 \geq s_0^2$ where s_0^2 is a fixed signal power.

Let $p(\mathbf{z})$ be the probability distribution of \mathbf{z} . The test concerns the hypothesis $p(\mathbf{z}) = p_0(\mathbf{z})$ against the alternative $p(\mathbf{z}) = p_1(\mathbf{z}, s^2)$ when $s^2 \geq s_0^2$. The test must take care of the most unfavorable situation which is $s^2 = s_0^2$. In testing this simple hypothesis against the simple alternative $p_0(\mathbf{z})$ there is a uniformly most powerful test, the likelihood ratio test. Denote with $f(\mathbf{z}, 0)$ and $f(\mathbf{z}, s^2)$ the density functions of \mathbf{z} for the distributions p_0 and p_1 . The test is based on the ratio $f(\mathbf{z}, s^2)/f(\mathbf{z}, 0)$ or some monotonic function thereof. Particularly we will take the logarithm.

Expressions for $f(\mathbf{z}, 0)$ and $f(\mathbf{z}, s_0)$ are easily derived. With no target present \mathbf{z} is normally distributed with covariance matrix C_M of order $M = 4m + 2$. Denote in partitioned form

$$C_M = \frac{1}{2}\sigma^2 \begin{bmatrix} A & B \\ B' & A \end{bmatrix}$$

with A and B square matrices of order $2m + 1$ and B' the transposed matrix B . Let (i, j) denote an arbitrary position in A or B and let i and j range over the index set $(1, \dots, 2m + 1)$. Then with $\zeta(\tau)$ and $\lambda(\tau)$ from (3)

$$A = \|\zeta[(j - i)T]\|, \quad B = \|\lambda[(j - i)T]\|$$

We find A to be real symmetric and B skew symmetric.

A target present, the return signal is made up of two additive and independent parts, one from the clutter (Eq. 2), and one from the target (Eq. 6), both of which are normally distributed. Independence of the target observations implies a covariance matrix of \mathbf{z} with a target present:

$$C_M + \frac{1}{2}s^2 D_M$$

D_M is a diagonal matrix of order M , conveniently partitioned into

$$D_M = \begin{bmatrix} D & 0 \\ 0 & D \end{bmatrix}$$

where D is diagonal of order $2m + 1$ with elements

$$d_i = G^2[\omega_a T(i - m - 1)], \quad i = 1, \dots, 2m + 1.$$

It follows

$$f(\mathbf{z}, 0) = C_1 \exp\{-\frac{1}{2}\mathbf{z}'C_M^{-1}\mathbf{z}\}$$

$$f(\mathbf{z}, s_0^2) = C_2 \exp\{-\frac{1}{2}\mathbf{z}'(C_M + \frac{1}{2}s_0^2 D_M)^{-1}\mathbf{z}\}$$

As test function we are led to consider

$$\zeta = \mathbf{z}'[C_M^{-1} - (C_M + \frac{1}{2}s_0^2 D_M)^{-1}]\mathbf{z}$$

The procedure is to decide a target is present if $\zeta > \zeta_0$ with ζ_0 conveniently chosen. We will develop the theory of threshold signal power based on the variable ζ .

11. THE VISIBILITY IN CLUTTER FOR THE TEST PROCEDURE

The signal power is now allowed to take on any positive value smaller or bigger than s_0^2 . Computation of $E_{p_0}\{\zeta\}$, $E_{p_0}\{\zeta^2\}$ and $E_{p_1}\{\zeta\}$ is simple although somewhat lengthy to carry out and we will be content to give the result. Let $F = s^2/\sigma^2$ and $F_0 = s_0^2/\sigma^2$ be the signal to clutter ratio and let

$$P = \sum_{i=1}^{2m+1} \frac{1}{\kappa_i(\kappa_i + F_0)}$$

$$Q = \sum_{i=1}^{2m+1} \frac{1}{(\kappa_i + F_0)^2}$$

Then the threshold signal inequality (12) reads

$$\frac{FP}{Q^{1/2}} \geq k$$

$\{\kappa_i\}_{i=1}^{2m+1}$ are the eigenvalues of the matrix $D^{-1}(A + C)$; the notations of A , B , and D are as in Section 10 and $C = (c_{ij})$ is constructed out of the matrix $B = (b_{ij})$ with the substitutions

$$c_{ij} = -b_{2m+2-i,j} = \lambda[(2m+2-j-i)T]$$

The visibility in clutter is $P/kQ^{1/2}$ measured in power ratio with $k = 9$. An application of Schwarz inequality shows the visibility to be equal or less than

$$\frac{1}{k} \left[\sum_{i=1}^{2m+1} \frac{1}{\kappa_i^2} \right]^{1/2} \quad (21)$$

with equality for $F_0 = 0$.

Once more suppose the radial velocity of the scatterers to be zero and also assume that there is no steady component in the return signal, that is, $a = 1$. The matrix C is then identically zero and the general element of A may be written

$$\zeta[(j-i)T] = \exp \left\{ -\frac{\pi}{4n^2} \eta^2(j-i)^2 \right\}, \quad i, j = 1, \dots, 2m+1$$

while that of D is

$$d_i = G^2[\omega_a T(i-m-1)] = \exp \left\{ -\frac{\pi}{n^2} (i-m-1)^2 \right\},$$

$$i = 1, \dots, 2m+1$$

When computing the eigenvalues of the matrix $D^{-1}A$ we might instead work with the symmetric matrix

$$U = \left(\frac{\xi[(j-i)T]}{\sqrt{d_i d_j}} \right), \quad i, j = 1, \dots, 2m+1$$

U is positive definite and thus has an inverse. The expression

$$\sum_{i=1}^{2m+1} \frac{1}{\kappa_i^2} \quad (22)$$

is identical to the trace of U^{-2} .

It appears from Fig. 6 that the test procedure with $m = 1$ already achieves a considerable gain compared to the MTI detector. With $m = 2$, the visibility is further improved and at $n = 5$ pulses per beamwidth, it ranges between 39 and 43 db for those values of n_p pictured in the figure. To illustrate the relation between the number of pulses treated coherently and the visibility we may, with $n = 5$ and $n_p = 250$, compare the normal radar, the MTI radar, and the test procedure for $m = 1$ and $m = 2$. The subclutter visibility is found to increase 12–15 db with each pulse added, the increase being greatest in a change from one to two pulses and then gradually decreasing. The curves in Fig. 6 do not all have the same trend when n becomes large because the addition of

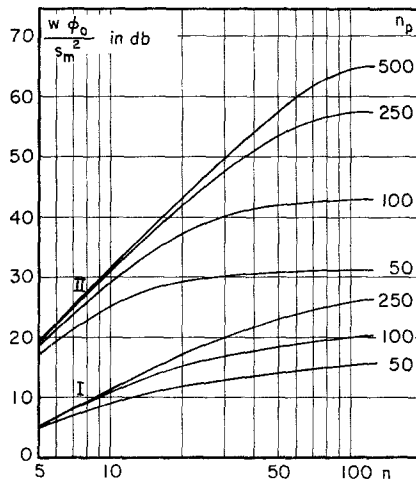


FIG. 6. Subclutter visibility versus number of hits per beamwidth when $a = 1$. I: MTI radar. II: test procedure $m = 1$, that is, three pulses coherently treated.

sweeps on the PPI gives the visibility a steady increase on the MTI radar only.

There are still many questions to answer with the generalized MTI detector. Each test procedure is here constructed with fixed statistical properties of the clutter signal, but it is expected that the procedure is sensitive to changes in these properties, especially with large m . In constructing a test function to handle a wide class of clutter signals, the assumption of a fixed density of clutter should be reconsidered. Another problem is the idealization $F_0 = 0$ which leads to the expression (21). The assumption implies in the limit a very small signal output from the detector but the presence of internal noise imposes the restriction $F_0 > 0$.

12. MTI RADAR WITH SCANNING ANTENNA BEAM

The performance of an MTI detector is usually limited by the antenna rotation and the change from one pulse to another of the clutter area illuminated. With the antenna rotating at a constant speed it is proposed to compensate for the antenna rotation with electronic scanning so that the antenna beam itself will be in a fixed position during n pulses. After one such sequence the beam jumps to a new position during one pulse interval. The first detector output after the change must be blanked from the PPI to secure proper operation of the subtraction circuits.

The beam scanning may be instrumented with ferrites by using their phase shifting properties. Employing a waveguide antenna, ferrites will be placed between each slot. The phase shift in one section should be varied linearly about 10° during 20 msec while the backscan should take less than 1 msec.

The ferrites may be thin slabs placed along the waveguide with a transversal magnetic field applied. Restrictions must be imposed on the arrangements of the slabs to secure identical phase shift for transmitted and received waves (Button and Lax, 1956). Recent investigations (Reggia and Spencer, 1957) explore the possibilities of ferrite rods centrally located in the waveguide and a weak longitudinal magnetic field applied, an arrangement which will be very convenient for our purpose.

REFERENCES

- BUTTON, K. J., AND LAX, B. (1956). Theory of ferrites in rectangular waveguides. *Trans. IRE AP-4*, 531-537.
- GRISETTI, R. S., SANTA, M. M., AND KIRKPATRICK, G. M. (1955). Effect of internal

- fluctuations and scanning on clutter attenuation in MTI radar. *Trans. IRE ANE-2*, 37-41.
- KERR, D. E. (1951). "Propagation of Short Radio Waves." McGraw-Hill, New York.
- LAWSON, J. L., AND UHLENBECK, G. E. (1950). "Threshold Signals." McGraw-Hill, New York.
- RCA Tube Handbook HB-3, Vols. 1 and 2.
- REGGIA, F., AND SPENCER, E. G. (1957). A new technique in ferrite phase shifting for beam scanning of microwave antennas. *Proc. I. R. E.* **45**, 1510-1517.
- RIDENOUR, L. N. (1947). "Radar System Engineering." McGraw-Hill, New York.
- SPONSLER, G. C., AND SHADER, F. L. (1954). PPI light spot brightness probability distributions. *J. Appl. Phys.* **25**, 1271-1277.